

Robust Management of Distributed Energy Resources for Microgrids with Renewables

Yu Zhang, *Student Member, IEEE*, Nikolaos Gatsis, *Student Member, IEEE*,
and Georgios B. Giannakis, *Fellow, IEEE*

Abstract—Due to its reduced communication overhead and robustness to failures, distributed energy management is of paramount importance in smart grids, especially in microgrids, which feature distributed generation (DG) and distributed storage (DS). Distributed economic dispatch for a microgrid with high renewable energy penetration and demand-side management operating in the grid-connected mode is considered in this paper. To address the intrinsically stochastic availability of renewable energy sources (RES), a novel power scheduling approach is introduced. The approach involves the actual renewable energy as well as the energy traded with the main grid, so that the supply-demand balance is maintained. The optimal scheduling strategy minimizes the microgrid net cost, which includes DG and DS costs, utility of dispatchable loads, and worst-case transaction cost stemming from the uncertainty in RES. Leveraging the dual decomposition, the optimization problem formulated is solved in a distributed fashion by the local controllers of DG, DS, and dispatchable loads. Numerical results are reported to corroborate the effectiveness of the novel approach.

Index Terms—Energy management, economic dispatch, demand side management, renewable energy, distributed energy resources, microgrids, robust optimization, distributed algorithms.

I. INTRODUCTION

Microgrids are power systems comprising distributed energy resources (DERs) and electricity end-users, possibly with controllable elastic loads, all deployed across a limited geographic area [1]. Depending on their origin, DERs can come either from distributed generation (DG) or from distributed storage (DS). DG refers to small-scale power generators such as diesel generators, fuel cells, and renewable energy sources (RES), as in wind or photovoltaic (PV) generation. DS paradigms include batteries, flywheels, and pumped storage. Specifically, DG brings power closer to the point it is consumed, thereby incurring fewer thermal losses and bypassing limitations imposed by a congested transmission network. Moreover, the increasing tendency towards high penetration of RES stems from their environment-friendly and price-competitive advantages over conventional generation. Typical microgrid loads include critical non-dispatchable types and also elastic controllable ones.

Microgrids also entail distribution networks with residential or commercial end-users, in rural or urban areas. A typical configuration is depicted in Fig. 1; see also [1]. The microgrid

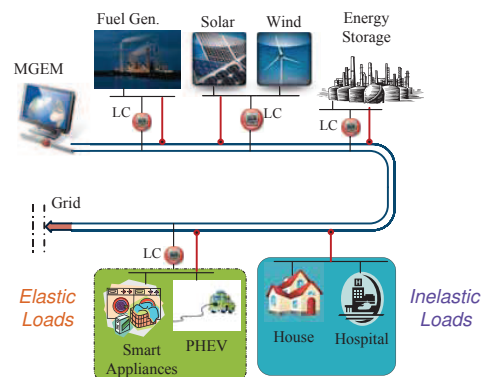


Fig. 1. Distributed control and computation architecture of a microgrid system. The microgrid energy manager (MGEM) coordinates the local controllers (LCs) of DERs and dispatchable loads.

energy manager (MGEM) coordinates the DERs and the controllable loads. Each of the DERs and loads has a local controller (LC), which coordinates with the MGEM the scheduling of resources through the communications infrastructure. The microgrid can operate in two modes: either connected or disconnected from the grid, the latter referred to as island mode.

In this context, the present paper deals with optimal energy management for both supply and demand of a microgrid incorporating RES. The microgrid is connected to the main grid, while energy can be sold to or purchased from the main grid. Decentralized algorithms are developed, which are robust to the uncertainty of the available RES. In addition to computationally efficient, distributed power scheduling must be resilient to communication outages or attacks. Furthermore, DER scheduling in microgrids must account for the variable and nondispatchable nature of the RES.

Optimal energy management for microgrids including economic dispatch (ED), unit commitment (UC), and demand-side management (DSM) is addressed in [2], but without pursuing a robust formulation against RES uncertainty. Mixed integer programming problems are formulated for microgrid scheduling and DSM in [3], [4]. Based on deterministic RES models (e.g., those relating wind power with wind speed), ED problems are investigated in [5] and [6]. In all the aforementioned works however, robust formulations accounting for the RES randomness are not pursued. Lyapunov stochastic optimization has been adopted to maximize the long-term profit of a RES facility in [7]. Stochastic programming is also used to cope with the variability of RES. Single-period chance-constrained ED problems for RES have been studied

This work is supported by NSF grant ECCS-1202135.

The authors are with the Department of Electrical and Computer Engineering, University of Minnesota, 200 Union Street SE, Minneapolis, MN 55455, USA. Tel/fax: +1(612)624-9510/625-2002. E-mails: {zhan1220, gatsisn, georgios}@umn.edu

in [8], yielding probabilistic guarantees that the load will be served. Considering the uncertainties of demand profiles and PV power generation, a stochastic program is formulated to minimize the overall cost of electricity and natural gas for a building in [9]. Without DSM, robust scheduling problems with penalty-based costs for uncertain supply and demand have been investigated in [10]. Recent works explore energy scheduling with DSM and RES using only centralized algorithms [11], [12]. An energy source control and DS planning problem for a small microgrid system is formulated and solved using model predictive control in [13]. Using energy storage to mitigate fluctuation in generation due to time-varying RES, an optimal power flow problem is formulated as a finite-horizon optimal control problem in [14]. Game-theoretic approaches for microgrids using (non-)cooperative and dynamic potential games are introduced in [15] and [16], respectively. Distributed algorithms are developed in [17], but they only coordinate DERs to supply a given load without considering the stochastic nature of RES. Similarly, robust energy management formulations have not been considered in the mentioned works [13]–[16].

This paper considers energy management of DERs and dispatchable loads with the goal of minimizing the microgrid net cost. The objective accounts for conventional DG cost, utility of elastic loads, penalized cost of DS, and a worst-case transaction cost. The latter stems from the ability of the microgrid to sell excess energy to the main grid, or to import energy in case of shortage. A *robust* formulation accounting for the worst-case amount of harvested RES is developed. A novel model is introduced in order to maintain the supply-demand balance arising from the intermittent RES. Moreover, a transaction-price-based condition is established to ensure convexity of the overall problem. The separable structure and strong duality of the resultant constrained problem are leveraged to develop a low-overhead *distributed* algorithm based on dual decomposition. The distributed implementation relies upon message exchanges between the MGEM and LCs. For faster convergence, the proximal bundle method is employed for the non-smooth subproblem handled by the LC of RES.

The rest of the paper is organized as follows. Section II formulates the robust energy management problem, and Section III develops its distributed solver. Numerical results are reported in Section IV, while conclusions and research outlook directions are provided in Section V.

Notation. Boldface lower case letters represent vectors; \mathbb{R}^n and \mathbb{R} stand for spaces of $n \times 1$ vectors and real numbers, respectively; \mathbb{R}_+^n is the n -dimensional non-negative orthant; \mathbf{x}' transpose, and $\|\mathbf{x}\|$ the Euclidean norm of \mathbf{x} .

II. ROBUST ENERGY MANAGEMENT FORMULATION

Consider a microgrid comprising M conventional (fossil fuel) generators, I RES facilities, and J DS devices (see also Fig. 1). The scheduling horizon is $\mathcal{T} := \{1, 2, \dots, T\}$ (e.g., one-day ahead). The particulars of the optimal scheduling problem are explained in the next subsections.

A. Load Demand Model

Loads are classified in two categories. The first comprises inelastic loads, whose power demand should be satisfied at all times. Examples are power requirements of hospitals or illumination demand from residential areas. The total fixed power demand from these critical loads at slot t is denoted by L^t .

The second category consists of elastic loads, which are dispatchable, in the sense that their power consumption is adjustable, and can be scheduled. These loads can be further divided in two subclasses, denoted respectively by \mathcal{K}_1 and \mathcal{K}_2 , each having the following characteristics:

- i) Class \mathcal{K}_1 contains loads with power consumption $P_{D_n}^t \in [P_{D_n}^{\min}, P_{D_n}^{\max}]$, where $n \in \mathcal{N} := \{1, \dots, N\}$, and $t \in \mathcal{T}$. Higher power consumption yields higher utility for the end user. The utility function of the n th dispatchable load, $U_{D_n}^t(P_{D_n}^t)$, is selected to be strictly increasing and concave, with typical choices being piecewise linear or smooth quadratic. An example from this class is an A/C unit.
- ii) Class \mathcal{K}_2 includes loads indexed by $q \in \mathcal{Q} := \{1, \dots, Q\}$ with power consumption limits $P_{E_q}^{\min}$ and $P_{E_q}^{\max}$, and prescribed total energy requirements E_q which have to be achieved from the start time S_q to termination time T_q . This type of loads can be the plug-in hybrid electric vehicles (PHEVs). Power demand variables $\{P_{E_q}^t\}_{t=1}^{T_q}$ therefore are constrained as $\sum_{t=S_q}^{T_q} P_{E_q}^t = E_q$ and $P_{E_q}^t \in [P_{E_q}^{\min,t}, P_{E_q}^{\max,t}]$, $t \in \mathcal{T}$, while $P_{E_q}^{\min,t} = P_{E_q}^{\max,t} = 0$ for $t \notin \{S_q, \dots, T_q\}$. Higher power consumption in earlier slots as opposed to later slots may be desirable for a certain load, so that the associated task finishes earlier. This behavior can be encouraged by adopting for the q th load an appropriately designed time-varying concave utility function $U_{E_q}^t(P_{E_q}^t)$. An example is $U_{E_q}^t(P_{E_q}^t) := \pi_q^t P_{E_q}^t$, with weights $\{\pi_q^t\}$ decreasing in t from slots S_q to T_q . Naturally, $U_{E_q}^t(P_{E_q}^t) \equiv 0$ can be selected if the consumer is indifferent to how power is consumed across slots.

B. Distributed Storage Model

Let B_j^t denote the state of charge (SoC) of the j th battery (i.e., the amount of energy storage) at the beginning of the slot t , with initial available energy B_j^0 while B_j^{\max} denotes the battery capacity, so that $0 \leq B_j^t \leq B_j^{\max}$, $j \in \mathcal{J} := \{1, \dots, J\}$. Let $P_{B_j}^t$ be the power delivered to (drawn from) the j th storage device at slot t , which amounts to charging ($P_{B_j}^t \geq 0$) or discharging ($P_{B_j}^t \leq 0$) of the battery. Clearly, the SoC obeys the dynamic equation

$$B_j^{t+1} = B_j^t + P_{B_j}^t, \quad j \in \mathcal{J}, \quad t \in \mathcal{T}. \quad (1)$$

Variables $P_{B_j}^t$ are constrained in the following ways:

- i) The amount of (dis)charging is bounded, that is

$$P_{B_j}^{\min} \leq P_{B_j}^t \leq P_{B_j}^{\max} \quad (2)$$

$$-\eta_j^{\text{dis}} B_j^t \leq P_{B_j}^t \leq \eta_j^{\text{ch}} (B_j^{\max} - B_j^t) \quad (3)$$

with bounds $P_{B_j}^{\min} < 0$ and $P_{B_j}^{\max} > 0$, while η_j^{ch} and η_j^{dis} are charging and discharging efficiencies; and

ii) Final SoC is also bounded, that is $B_j^T \geq B_j^{\min}$.

The storage cost $H_j^t(B_j^t)$ can be also taken into account. Considering the battery reserve, a penalty can be postulated proportional to the deviation from the battery capacity as $H_j^t(B_j^t) := \varpi_j^t(B_j^{\max} - B_j^t)$, meaning it is desirable to maintain a close-to-full battery level at the end of each period [14].

C. Worst-case Transaction Cost

Let W_i^t denote the *actual* renewable energy harvested by the i th RES facility at time slot t , and also let \mathbf{w} collect all W_i^t , i.e., $\mathbf{w} := [W_1^1, \dots, W_1^T, \dots, W_I^1, \dots, W_I^T]$. To capture the intrinsically stochastic and time-varying availability of RES, it is postulated that \mathbf{w} is unknown, but lies in a polyhedral uncertainty set \mathcal{W} . The following are two practical examples of uncertainty sets.

i) The first example postulates a separate uncertainty set \mathcal{W}_i for each RES facility in the form

$$\mathcal{W}_i := \left\{ \{W_i^t\}_{t=1}^T \mid \underline{W}_i^t \leq W_i^t \leq \overline{W}_i^t, \right. \\ \left. W_{i,s}^{\min} \leq \sum_{t \in \mathcal{T}_{i,s}} W_i^t \leq W_{i,s}^{\max}, \mathcal{T} = \bigcup_{s=1}^S \mathcal{T}_{i,s} \right\} \quad (4)$$

where \underline{W}_i^t (\overline{W}_i^t) denotes a lower (upper) bound on W_i^t ; time horizon \mathcal{T} is partitioned into consecutive but non-overlapping sub-horizons $\mathcal{T}_{i,s}$ for $i = 1, \dots, I$, $s = 1, 2, \dots, S$; the total renewable energy for the i th RES facility over the s th sub-horizon is assumed bounded by $W_{i,s}^{\min}$ and $W_{i,s}^{\max}$. In this example, uncertainty set \mathcal{W} takes the form of Cartesian product

$$\mathcal{W} = \mathcal{W}_1 \times \dots \times \mathcal{W}_I. \quad (5)$$

ii) The second example assumes a joint uncertainty model across all the RES facilities as

$$\mathcal{W} := \left\{ \mathbf{w} \mid \underline{W}_i^t \leq W_i^t \leq \overline{W}_i^t, \right. \\ \left. W_s^{\min} \leq \sum_{t \in \mathcal{T}_s} \sum_{i=1}^I W_i^t \leq W_s^{\max}, \mathcal{T} = \bigcup_{s=1}^S \mathcal{T}_s \right\} \quad (6)$$

where \underline{W}_i^t (\overline{W}_i^t) denotes a lower (upper) bound on W_i^t ; time horizon \mathcal{T} is partitioned into consecutive but non-overlapping sub-horizons \mathcal{T}_s for $s = 1, 2, \dots, S$; the total renewable energy harvested by all the RES facilities over the s th sub-horizon is bounded by W_s^{\min} and W_s^{\max} ; see also [12].

The previous two RES uncertainty models are quite general and can take into account different geographical and meteorological factors. The only information required is these deterministic lower and upper bounds, namely $\underline{W}_i^t, \overline{W}_i^t, W_{i,s}^{\min}, W_{i,s}^{\max}, W_s^{\min}, W_s^{\max}$, which can be determined via inference schemes based on historical data [18].

Supposing the microgrid operates in a grid-connected mode, a transaction mechanism between the microgrid and the main grid is present, whereby the microgrid can buy/sell energy

from/to the spot market. Let P_R^t be an auxiliary variable denoting the net power delivered to the microgrid from the renewable energy sources and the distributed storage in order to maintain the supply-demand balance at slot t . The shortage energy per slot t is given by $\left[P_R^t - \sum_{i=1}^I W_i^t + \sum_{j=1}^J P_{B_j}^t \right]^+$, while the surplus energy is $\left[P_R^t - \sum_{i=1}^I W_i^t + \sum_{j=1}^J P_{B_j}^t \right]^-$, where $[a]^+ := \max\{a, 0\}$, and $[a]^- := \max\{-a, 0\}$.

The amount of shortage energy is bought with known purchase price α^t , while the surplus energy is sold to the main grid with known selling price β^t . The worst-case net transaction cost is thus given by

$$G(\{P_R^t\}, \{P_{B_j}^t\}) := \max_{\mathbf{w} \in \mathcal{W}} \sum_{t=1}^T \left(\alpha^t \left[P_R^t - \sum_{i=1}^I W_i^t + \sum_{j=1}^J P_{B_j}^t \right]^+ \right. \\ \left. - \beta^t \left[P_R^t - \sum_{i=1}^I W_i^t + \sum_{j=1}^J P_{B_j}^t \right]^- \right) \quad (7)$$

where $\{P_R^t\}$ collects P_R^t for $t = 1, 2, \dots, T$ and $\{P_{B_j}^t\}$ collects $P_{B_j}^t$ for $j = 1, 2, \dots, J$, $t = 1, 2, \dots, T$.

Remark 1. (Stochastic model). Instead of the worst-case robust model advocated here, a probabilistic approach is also possible. Specifically, suppose that W_i^t is a function of a random quantity v_i^t . In the case of wind generation, v_i^t is the wind velocity, for which different models are available, and the mapping $W_i^t(v_i^t)$ is known [19]. Due to power shortage, the expected purchase cost becomes $G(\{P_R^t\}, \{P_{B_j}^t\}) := \sum_{t=1}^T \alpha^t \mathbb{E}_{\mathbf{v}} [P_R^t - \sum_{i=1}^I W_i^t(v_i^t) + \sum_{j=1}^J P_{B_j}^t]^+$, where $\mathbf{v}^t := [v^1, \dots, v^T]$. Likewise, the expected revenue can be obtained by averaging $[P_R^t - \sum_{i=1}^I W_i^t(v_i^t) + \sum_{j=1}^J P_{B_j}^t]^-$ over t . This stochastic model is useful when statistical knowledge for the RES is available, as when \mathbf{v} stands for the wind velocity, which typically satisfies the Weibull distribution [19].

D. Microgrid Energy Management Problem

Apart from RES, microgrids typically entail also conventional DG. Let $P_{G_m}^t$ be the power produced by the m th conventional generator, where $m \in \mathcal{M} := \{1, \dots, M\}$ and $t \in \mathcal{T}$. The cost of the m th conventional generator is given by a strictly increasing and convex function $C_m^t(P_{G_m}^t)$. Typically, the chosen $C_m^t(P_{G_m}^t)$ is either piecewise linear or smooth quadratic.

The energy management problem amounts to minimizing the microgrid social net cost; that is, the cost of conventional generation, storage, as well as the worst-case transaction cost (due to the volatility of RES) minus the utility of dispatchable loads:

$$(P1) \quad \min_{\substack{\{P_{G_m}^t, P_{D_n}^t, \\ P_{E_q}^t, P_{B_j}^t, P_R^t\}}} \sum_{t=1}^T \left(\sum_{m=1}^M C_m^t(P_{G_m}^t) - \sum_{n=1}^N U_{D_n}^t(P_{D_n}^t) \right. \\ \left. - \sum_{q=1}^Q U_{E_q}^t(P_{E_q}^t) + \sum_{j=1}^J H_j^t(B_j^t) \right) + G(\{P_R^t\}, \{P_{B_j}^t\}) \quad (8a)$$

subject to:

$$P_{G_m}^{\min} \leq P_{G_m}^t \leq P_{G_m}^{\max}, \quad m \in \mathcal{M}, \quad t \in \mathcal{T} \quad (8b)$$

$$P_{G_m}^t - P_{G_m}^{t-1} \leq R_{m,\text{up}}, \quad m \in \mathcal{M}, \quad t \in \mathcal{T} \quad (8c)$$

$$P_{G_m}^{t-1} - P_{G_m}^t \leq R_{m,\text{down}}, \quad m \in \mathcal{M}, \quad t \in \mathcal{T} \quad (8d)$$

$$\sum_{m=1}^M (P_{G_m}^{\max} - P_{G_m}^t) \geq \text{SR}^t, \quad t \in \mathcal{T} \quad (8e)$$

$$P_{D_n}^{\min} \leq P_{D_n}^t \leq P_{D_n}^{\max}, \quad n \in \mathcal{N}, \quad t \in \mathcal{T} \quad (8f)$$

$$P_{E_q}^{\min,t} \leq P_{E_q}^t \leq P_{E_q}^{\max,t}, \quad q \in \mathcal{Q}, \quad t \in \mathcal{T} \quad (8g)$$

$$\sum_{t=S_q}^{T_q} P_{E_q}^t = E_q, \quad q \in \mathcal{Q}, \quad (8h)$$

$$0 \leq B_j^t \leq B_j^{\max}, \quad j \in \mathcal{J}, \quad t \in \mathcal{T} \quad (8i)$$

$$P_{B_j}^{\min} \leq P_{B_j}^t \leq P_{B_j}^{\max}, \quad j \in \mathcal{J}, \quad t \in \mathcal{T} \quad (8j)$$

$$-\eta_j^{\text{dis}} B_j^t \leq P_{B_j}^t \leq \eta_j^{\text{ch}} (B_j^{\max} - B_j^t), \quad j \in \mathcal{J}, \quad t \in \mathcal{T} \quad (8k)$$

$$B_j^{t+1} = B_j^t + P_{B_j}^t, \quad j \in \mathcal{J}, \quad t \in \mathcal{T} \quad (8l)$$

$$B_j^T \geq B_j^{\min}, \quad t \in \mathcal{T} \quad (8m)$$

$$P_R^{\min} \leq P_R^t \leq P_R^{\max}, \quad t \in \mathcal{T} \quad (8n)$$

$$\sum_{m=1}^M P_{G_m}^t + P_R^t = L^t + \sum_{n=1}^N P_{D_n}^t + \sum_{q=1}^Q P_{E_q}^t, \quad t \in \mathcal{T}. \quad (8o)$$

Constraints (8b)–(8e) stand for the minimum/maximum power output, ramping up/down limits, and spinning reserves, respectively, which capture the typical physical requirements of a power generation system. Constraints (8f) and (8n) correspond to the minimum/maximum power of the flexible load demand and committed renewable energy. Constraint (8o) is the power supply-demand *balance equation* ensuring the total demand is satisfied by the power generation at any time.

Note that constraints (8b)–(8o) are linear, while $C_m^t(\cdot)$, $-U_{D_n}^t(\cdot)$, $H_j^t(\cdot)$, and $-U_{E_q}^t(\cdot)$ are convex (possibly non-differentiable or non-strictly convex) functions. Consequently, the convexity of (P1) depends on that of $G(\{P_R^t\}, \{P_{B_j}^t\})$, which is established in the following proposition.

Proposition 1. *If the selling price β^t does not exceed the purchase price α^t for any $t \in \mathcal{T}$, then the worst-case transaction cost $G(\{P_R^t\}, \{P_{B_j}^t\})$ is convex in $\{P_R^t\}$ and $\{P_{B_j}^t\}$.*

Proof: Using that $[a]^+ + [a]^- = |a|$, and $[a]^+ - [a]^- = a$, $G(\{P_R^t\}, \{P_{B_j}^t\})$ can be re-written as

$$G(\{P_R^t\}, \{P_{B_j}^t\}) = \max_{\mathbf{w} \in \mathcal{W}} \sum_{t=1}^T \left(\delta^t \left| P_R^t - \sum_{i=1}^I W_i^t + \sum_{j=1}^J P_{B_j}^t \right| + \gamma^t (P_R^t - \sum_{i=1}^I W_i^t + \sum_{j=1}^J P_{B_j}^t) \right) \quad (9)$$

with $\delta^t := (\alpha^t - \beta^t)/2$, and $\gamma^t := (\alpha^t + \beta^t)/2$. Since the absolute value function is convex, and the operations of nonnegative weighted summation and pointwise maximum (over an infinite set) preserve convexity [20, Sec. 3.2], the claim follows readily. ■

An immediate corollary of Proposition 1 is that the energy management problem (P1) is convex if $\beta^t \leq \alpha^t$ for all t . The next section focuses on this case, and designs an efficient decentralized solver for (P1).

III. DISTRIBUTED ALGORITHM

In order to facilitate a distributed algorithm for (P1), a variable transformation is useful. Specifically, upon introducing $\tilde{P}_R^t := P_R^t + \sum_{j=1}^J P_{B_j}^t$, (P1) can be re-written as

$$(P2) \quad \min_{\mathbf{x}} \sum_{t=1}^T \left(\sum_{m=1}^M C_m^t(P_{G_m}^t) - \sum_{n=1}^N U_{D_n}^t(P_{D_n}^t) - \sum_{q=1}^Q U_{E_q}^t(P_{E_q}^t) + \sum_{j=1}^J H_j^t(B_j^t) \right) + G(\{\tilde{P}_R^t\}) \quad (10a)$$

subject to: (8b)–(8o)

$$\tilde{P}_R^t = P_R^t + \sum_{j=1}^J P_{B_j}^t, \quad t \in \mathcal{T} \quad (10b)$$

where \mathbf{x} collects all the primal variables $\{P_{G_m}^t, P_{D_n}^t, P_{E_q}^t, P_{B_j}^t, B_j^t, P_R^t, \tilde{P}_R^t\}$; $\{\tilde{P}_R^t\}$ collects \tilde{P}_R^t for $t = 1, \dots, T$; and

$$G(\{\tilde{P}_R^t\}) := \max_{\mathbf{w} \in \mathcal{W}} \sum_{t=1}^T \left(\delta^t \left| \tilde{P}_R^t - \sum_{i=1}^I W_i^t \right| + \gamma^t (\tilde{P}_R^t - \sum_{i=1}^I W_i^t) \right). \quad (11)$$

The following proposition extends the result of Proposition 1 to the transformed problem, and asserts its strong duality.

Proposition 2. *If (P2) is feasible, and the selling price β^t does not exceed the purchase price α^t for any $t \in \mathcal{T}$, then there is no duality gap.*

Proof: Due to the strong duality theorem for the optimization problems with linear constraints (cf. [21, Prop. 5.2.1]), it suffices to show that the cost function is convex over the entire space and its optimal value is finite. First, using the same argument, convexity of $G(\{\tilde{P}_R^t\})$ in $\{\tilde{P}_R^t\}$ is immediate under the transaction price condition. The finiteness of the optimal value is guaranteed by the fact that the continuous convex cost (10a) is minimized over a nonempty compact set specified by (8b)–(8o), and (10b). ■

The strong duality asserted by Proposition 2 motivates the use of Lagrangian relaxation techniques in order to solve the scheduling problem. Moreover, problem (P2) is clearly separable, meaning that its cost and constraints are sums of terms, with each term dependent on different variables, namely $\{P_{G_m}^t\}$, $\{P_{D_n}^t\}$, $\{P_{E_q}^t\}$, $\{B_j^t\}$, $\{P_R^t\}$ and $\{\tilde{P}_R^t\}$. The features of strong duality and separability then imply that Lagrangian relaxation and dual decomposition are applicable to yield a decentralized algorithm; see also related techniques in the power systems [22] and communication networks [23]. Coordinated by dual variables, the dual approach decomposes the original problem into several separate subproblems that can be solved by the LCs in parallel. The development of the distributed algorithm is undertaken next.

A. Dual Decomposition

Constraints (8e), (8o), and (10b) couple variables across generators, loads, and the RES. Let \mathbf{z} collect dual variables $\{\mu^t\}$, $\{\lambda^t\}$, and $\{\nu^t\}$, which denote the corresponding Lagrange multipliers. Keeping the remaining constraints implicit, the partial Lagrangian is given by

$$\begin{aligned} \mathcal{L}(\mathbf{x}, \mathbf{z}) = & \sum_{t=1}^T \left(\sum_{m=1}^M C_m^t(P_{G_m}^t) - \sum_{n=1}^N U_{D_n}^t(P_{D_n}^t) \right. \\ & \left. - \sum_{q=1}^Q U_{E_q}^t(P_{E_q}^t) + \sum_{j=1}^J H_j^t(B_j^t) \right) + G(\{\tilde{P}_R^t\}) \\ & + \sum_{t=1}^T \left\{ \mu^t \left(\text{SR}^t - \sum_{m=1}^M (P_{G_m}^{\max} - P_{G_m}^t) \right) \right. \\ & - \lambda^t \left(\sum_{m=1}^M P_{G_m}^t + P_R^t - \sum_{n=1}^N P_{D_n}^t - \sum_{q=1}^Q P_{E_q}^t - L^t \right) \\ & \left. - \nu^t \left(\tilde{P}_R^t - P_R^t - \sum_{j=1}^J P_{B_j}^t \right) \right\}. \end{aligned} \quad (12)$$

Then, the dual function can be written as

$$\begin{aligned} \mathcal{D}(\mathbf{z}) = \min_{\mathbf{x}} \mathcal{L}(\mathbf{x}, \mathbf{z}) \\ \text{s.t. (8b) - (8d), (8f) - (8n)} \end{aligned}$$

and the dual problem is given by

$$\max \mathcal{D}(\{\mu^t\}, \{\lambda^t\}, \{\nu^t\}) \quad (13a)$$

$$\text{s.t. } \mu^t \geq 0, \lambda^t, \nu^t \in \mathbb{R}, t \in \mathcal{T}. \quad (13b)$$

The subgradient method will be employed to obtain the optimal multipliers and power schedules. The iterative process is described next, followed by its distributed implementation.

1) *Subgradient Iterations:* The subgradient method amounts to running the recursions [24, Sec. 6.3]

$$\mu^t(k+1) = [\mu^t(k) + ag_{\mu^t}(k)]^+ \quad (14a)$$

$$\lambda^t(k+1) = \lambda^t(k) + ag_{\lambda^t}(k) \quad (14b)$$

$$\nu^t(k+1) = \nu^t(k) + ag_{\nu^t}(k) \quad (14c)$$

where k is the iteration index; $a > 0$ is a constant stepsize; while $g_{\mu^t}(k)$, $g_{\lambda^t}(k)$, and $g_{\nu^t}(k)$ denote the subgradients of the dual function with respect to $\mu^t(k)$, $\lambda^t(k)$, and $\nu^t(k)$, respectively. These subgradients can be expressed in the following simple forms

$$g_{\mu^t}(k) = \text{SR}^t - \sum_{m=1}^M (P_{G_m}^{\max} - P_{G_m}^t(k)) \quad (15a)$$

$$\begin{aligned} g_{\lambda^t}(k) = & L^t + \sum_{n=1}^N P_{D_n}^t(k) + \sum_{q=1}^Q P_{E_q}^t(k) \\ & - \sum_{m=1}^M P_{G_m}^t(k) - P_R^t(k) \end{aligned} \quad (15b)$$

$$g_{\nu^t}(k) = P_R^t(k) + \sum_{j=1}^J P_{B_j}^t(k) - \tilde{P}_R^t(k) \quad (15c)$$

where $P_{G_m}^t(k)$, $P_{D_n}^t(k)$, $P_{E_q}^t(k)$, $P_{B_j}^t(k)$, $P_R^t(k)$, and $\tilde{P}_R^t(k)$ are given by (16)–(20).

Iterations are initialized with arbitrary $\lambda^t(0), \nu^t(0) \in \mathbb{R}$, and $\mu^t(0) \geq 0$. The iterates are guaranteed to converge to a neighborhood of the optimal multipliers [24, Sec. 6.3]. The size of the neighborhood is proportional to the stepsize, and can therefore be controlled by the stepsize.

When the primal objective is *not* strictly convex, a primal averaging procedure is necessary to obtain the optimal power schedules, which are then given by

$$\bar{\mathbf{x}}(k) = \frac{1}{k} \sum_{j=0}^{k-1} \mathbf{x}(j) = \frac{1}{k} \mathbf{x}(k-1) + \frac{k-1}{k} \bar{\mathbf{x}}(k-1). \quad (21)$$

$$\{P_{G_m}^t(k)\}_{t=1}^T \in \arg \min_{\{P_{G_m}^t\}} \left\{ \sum_{t=1}^T \left(C_m^t(P_{G_m}^t) + (\mu^t(k) - \lambda^t(k)) P_{G_m}^t \right) \right\} \quad (16)$$

s.t. (8b)–(8d)

$$\{P_{D_n}^t(k)\}_{t=1}^T \in \arg \min_{\{P_{D_n}^t\}} \left\{ \sum_{t=1}^T \left(\lambda^t(k) P_{D_n}^t - U_{D_n}^t(P_{D_n}^t) \right) \right\} \quad (17)$$

s.t. (8f)

$$\{P_{E_q}^t(k)\}_{t=1}^T \in \arg \min_{\{P_{E_q}^t\}} \left\{ \sum_{t=1}^T \left(\lambda^t(k) P_{E_q}^t - U_{E_q}^t(P_{E_q}^t) \right) \right\} \quad (18)$$

s.t. (8g)–(8h)

$$\{P_{B_j}^t(k)\}_{t=1}^T \in \arg \min_{\{P_{B_j}^t, B_j^t\}} \left\{ \sum_{t=1}^T \left(\nu^t(k) P_{B_j}^t + H_j^t(B_j^t) \right) \right\} \quad (19)$$

s.t. (8i)–(8m)

$$\{P_R^t(k), \tilde{P}_R^t(k)\}_{t=1}^T \in \arg \min_{\substack{\{P_R^t\} \text{ s.t. (8n),} \\ \tilde{P}_R^t \in \mathbb{R}^T}} \left\{ \sum_{t=1}^T \left((\nu^t(k) - \lambda^t(k)) P_R^t \right) + G(\{\tilde{P}_R^t\}) - \sum_{t=1}^T \nu^t(k) \tilde{P}_R^t \right\} \quad (20)$$

The running averages can be recursively computed as in (21), and are also guaranteed to converge to a neighborhood of the optimal solution [25]. Note that other convergence-guaranteed stepsize rules (e.g., diminishing stepsize) and primal averaging (weights proportional to the stepsize) can also be utilized; see [26] for detailed discussions.

2) *Distributed Implementation*: The form of the subgradient iterations easily lends itself to a distributed implementation utilizing the control and communication capabilities of a typical microgrid.

Specifically, the MGEM maintains and updates the Lagrange multipliers via (14). The LCs of conventional generation, dispatchable loads, storage devices, and RES solve subproblems (16)–(20), respectively. These subproblems can be solved if the MGEM sends the current multiplier iterates $\mu^t(k)$, $\lambda^t(k)$, and $\nu^t(k)$ to the LCs. The LCs send back to the MGEM the quantities $\sum_{m=1}^M P_{G_m}^t(k)$, $\sum_{n=1}^N P_{D_n}^t(k)$, $\sum_{q=1}^Q P_{E_q}^t(k)$, $\sum_{j=1}^J P_{B_j}^t(k)$, $P_R^t(k)$, and $\tilde{P}_R^t(k)$ which are in turn used to form the subgradients according to (15). The distributed algorithm using dual decomposition is tabulated as Algorithm 1, and the interactive process of message passing is illustrated in Fig. 2.

Algorithm 1 Distributed energy management algorithm

- 1: Initialize Lagrange multipliers $\lambda^t = \mu^t = \nu^t = 0$
 - 2: **repeat** ($k = 0, 1, 2, \dots$)
 - 3: **for** $t = 1, 2, \dots, T$ **do**
 - 4: Broadcast $\lambda^t(k)$, $\mu^t(k)$, and $\nu^t(k)$ to LCs of conventional generators, controllable loads, storage devices, and RES facilities
 - 5: Update power scheduling $P_{G_m}^t(k)$, $P_{D_n}^t(k)$, $P_{E_q}^t(k)$, $P_{B_j}^t(k)$, $P_R^t(k)$, and $\tilde{P}_R^t(k)$ by solving (16)–(20)
 - 6: Update $\lambda^t(k)$, $\mu^t(k)$, and $\nu^t(k)$ via (14)
 - 7: **end for**
 - 8: Running averages of primal variables via (21)
 - 9: **until** Convergence
-

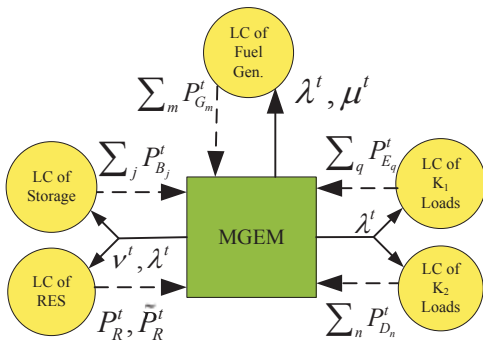


Fig. 2. Decomposition and message exchange.

B. Solving the LC Subproblems

This subsection shows how to solve each subproblem (16)–(20). Specifically, $C_m^t(\cdot)$, $-U_{D_n}^t(\cdot)$, $-U_{E_q}^t(\cdot)$, and $H_j^t(\cdot)$ are chosen either convex piece-wise linear or smooth convex

quadratic. Correspondingly, the first four subproblems (16)–(19) are essentially linear programs (LPs) or quadratic programs (QPs), which can be solved efficiently. Therefore, the main focus is on solving (20).

The optimal solution of $P_R^t(k)$ in (20) is easy to obtain as

$$P_R^t(k) = \begin{cases} P_R^{\min}, & \text{if } \nu^t(k) \geq \lambda^t(k) \\ P_R^{\max}, & \text{if } \nu^t(k) < \lambda^t(k). \end{cases} \quad (22)$$

However, due to the absolute value operator and the maximization over \mathbf{w} in the definition of $G(\{\tilde{P}_R^t\})$, subproblem (20) is a convex nondifferentiable problem in $\{\tilde{P}_R^t\}$, which can be challenging to solve. As a state-of-the-art technique for convex nondifferentiable optimization problems [27], [24, Ch. 6], the bundle method is employed to obtain $\{\tilde{P}_R^t(k)\}$.

Upon defining

$$\tilde{G}(\{\tilde{P}_R^t\}) := G(\{\tilde{P}_R^t\}) - \sum_{t=1}^T \nu^t(k) \tilde{P}_R^t \quad (23)$$

the subgradient of $\tilde{G}(\{\tilde{P}_R^t\})$ with respect to \tilde{P}_R^t needed for the bundle method can be obtained by the generalization of Danskin's Theorem [24, Sec. 6.3] as

$$\partial \tilde{G}(\{\tilde{P}_R^t\}) = \begin{cases} \alpha^t - \lambda^t - \nu^t, & \text{if } \tilde{P}_R^t \geq \sum_{i=1}^I (W_i^t)^* \\ \beta^t - \lambda^t - \nu^t, & \text{if } \tilde{P}_R^t < \sum_{i=1}^I (W_i^t)^* \end{cases} \quad (24)$$

where for given $\{\tilde{P}_R^t\}$ it holds that

$$\mathbf{w}^* \in \arg \max_{\mathbf{w} \in \mathcal{W}} \left\{ \sum_{t=1}^T \left(\delta^t |\tilde{P}_R^t - \sum_{i=1}^I W_i^t| + \gamma^t (\tilde{P}_R^t - \sum_{i=1}^I W_i^t) \right) \right\}. \quad (25)$$

With $\mathbf{p} := [\tilde{P}_R^1, \dots, \tilde{P}_R^T]$, the bundle method generates a sequence $\{\mathbf{p}_\ell\}$ with guaranteed convergence to the optimal $\{\tilde{P}_R^t(k)\}$; see e.g., [27], [24, Ch. 6]. The iterate $\mathbf{p}_{\ell+1}$ is obtained by minimizing a polyhedral approximation of $\tilde{G}(\mathbf{p})$ with a quadratic proximal regularization as follows

$$\mathbf{p}_{\ell+1} := \arg \min_{\mathbf{p} \in \mathbb{R}^T} \left\{ \hat{G}_\ell(\mathbf{p}) + \frac{\rho_\ell}{2} \|\mathbf{p} - \mathbf{y}_\ell\|^2 \right\} \quad (26)$$

where $\hat{G}_\ell(\mathbf{p}) := \max\{\tilde{G}(\mathbf{p}_0) + \mathbf{g}'_0(\mathbf{p} - \mathbf{p}_0), \dots, \tilde{G}(\mathbf{p}_\ell) + \mathbf{g}'_\ell(\mathbf{p} - \mathbf{p}_\ell)\}$; \mathbf{g}_ℓ is the subgradient of $\tilde{G}(\mathbf{p})$ evaluated at the point $\mathbf{p} = \mathbf{p}_\ell$, which is calculated according to (24); proximity weight ρ_ℓ is to control stability of the iterates; and the proximal center \mathbf{y}_ℓ is updated according to a query for descent

$$\mathbf{y}_{\ell+1} = \begin{cases} \mathbf{p}_{\ell+1}, & \text{if } \tilde{G}(\mathbf{y}_\ell) - \tilde{G}(\mathbf{p}_{\ell+1}) \geq \theta \eta_\ell \\ \mathbf{y}_\ell, & \text{otherwise} \end{cases} \quad (27)$$

where $\eta_\ell = \tilde{G}(\mathbf{y}_\ell) - \left(\hat{G}_\ell(\mathbf{p}_{\ell+1}) + \frac{\rho_\ell}{2} \|\mathbf{p}_{\ell+1} - \mathbf{y}_\ell\|^2 \right)$, $\theta \in (0, 1)$.

It is worth mentioning that (26) is essentially a QP over a simplex in the dual space, which is efficiently solvable by practical optimization algorithms. The corresponding transformation is shown in Appendix I for the interested readers.

Algorithms for solving (25) depend on the form of the uncertainty set \mathcal{W} , and are elaborated next.

C. Vertex Enumerating Algorithms

In order to obtain \mathbf{w}^* , the convex nondifferentiable function in (25) should be maximized over \mathcal{W} . This is generally an NP-hard convex maximization problem. However, for the specific problem here, the special structure of the problem can be utilized to obtain a computationally efficient approach.

Specifically, the global solution is attained at the extreme points of the polytope [24, Sec. 2.4]. Therefore, the objective in (25) can be evaluated at all vertices of \mathcal{W} to obtain the global solution. Since there are only finitely many vertices, (25) can be solved in a *finite* number of steps.

For the polytopes \mathcal{W} with special structure [cf. (4), (6)], characterizations of vertices are established in Propositions 3 and 4. Capitalizing on these propositions, vertex enumerating procedures are designed consequently, and are tabulated as Algorithms 2 and 3.

Proposition 3. *For a polytope $\mathcal{A} := \{\mathbf{a} \in \mathbb{R}^n | \underline{\mathbf{a}} \preceq \mathbf{a} \preceq \bar{\mathbf{a}}, a^{\min} \leq \mathbf{1}'\mathbf{a} \leq a^{\max}\}$, $\mathbf{a}^v \in \mathcal{A}$ is a vertex (extreme point) of \mathcal{A} if and only if it has one of the following forms: i) $a_i^v = \underline{a}_i$ or \bar{a}_i for $i = 1, \dots, n$; or ii) $a_i^v = a^{\min} - \sum_{j \neq i} a_j^v$ or $a^{\max} - \sum_{j \neq i} a_j^v$, $a_j^v = \underline{a}_j$ or \bar{a}_j , for $i, j = 1, \dots, n, j \neq i$.*

Proof: See Appendix II-A. ■

Essentially, Proposition 3 verifies the geometric characterization of vertices. Since \mathcal{W} is the part of a hyperrectangle (orthotope) between two parallel hyperplanes, its vertices can only either be the hyperrectangle's vertices which are not cut away, or, the vertices of the intersections of the hyperrectangle and the hyperplanes, which must appear in some edges of the hyperrectangle.

Next, the vertex characterization of a polytope in a Cartesian product formed by many lower-dimensional polytopes like \mathcal{A} is established, which is needed for the uncertainty set (4).

Proposition 4. *Assume $\mathbf{b} \in \mathbb{R}^n$ is divided into S consecutive and non-overlapping blocks as $\mathbf{b} = [\mathbf{b}'_1, \dots, \mathbf{b}'_S]'$, where $\mathbf{b}_s \in \mathbb{R}^{n_s}$ and $\sum_{s=1}^S n_s = n$. Consider a polytope $\mathcal{B} := \{\mathbf{b} \in \mathbb{R}^n | \underline{\mathbf{b}} \preceq \mathbf{b} \preceq \bar{\mathbf{b}}, b_s^{\min} \leq \mathbf{1}'_s \mathbf{b}_s \leq b_s^{\max}, s = 1, \dots, S\}$. Then $\mathbf{b}^v = [(\mathbf{b}'_1)^v, \dots, (\mathbf{b}'_S)^v]'$ is a vertex of \mathcal{B} if and only if for $s = 1, \dots, S$, \mathbf{b}_s^v is the vertex of a lower-dimensional polytope $\mathcal{B}_s := \{\mathbf{b}_s \in \mathbb{R}^{n_s} | \underline{\mathbf{b}}_s \preceq \mathbf{b}_s \preceq \bar{\mathbf{b}}_s, b_s^{\min} \leq \mathbf{1}'_s \mathbf{b}_s \leq b_s^{\max}\}$.*

Proof: See Appendix II-B. ■

Algorithm 2 Enumerate all the vertices of a polytope \mathcal{A}

- 1: Initialize vertex set $\mathcal{V} = \emptyset$
 - 2: Generate set $\hat{\mathcal{A}} := \{\hat{\mathbf{a}} \in \mathbb{R}^n | \hat{a}_i = \underline{a}_i \text{ or } \bar{a}_i, i = 1, \dots, n\}$; check the feasibility of all the points in set $\hat{\mathcal{A}}$, i.e., if $a^{\min} \leq \mathbf{1}'\hat{\mathbf{a}} \leq a^{\max}$, then $\mathcal{V} = \mathcal{V} \cup \{\hat{\mathbf{a}}\}$
 - 3: Generate set $\hat{\mathcal{A}} := \{\hat{\mathbf{a}} \in \mathbb{R}^n | \hat{a}_i = a^{\min} - \sum_{j \neq i} \hat{a}_j \text{ or } a^{\max} - \sum_{j \neq i} \hat{a}_j, \hat{a}_j = \underline{a}_j \text{ or } \bar{a}_j, i, j = 1, \dots, n, j \neq i\}$; check the feasibility of all the points in set $\hat{\mathcal{A}}$, i.e., if $\underline{\mathbf{a}} \preceq \hat{\mathbf{a}} \preceq \bar{\mathbf{a}}$, then $\mathcal{V} = \mathcal{V} \cup \{\hat{\mathbf{a}}\}$
-

Algorithms 2 and 3 can be used to generate the vertices of uncertainty sets (4) and (6) as described next.

- i) For uncertainty set (4), first use Algorithm 2 to obtain the vertices corresponding to each sub-horizon $\mathcal{T}_{i,s}$ for

Algorithm 3 Enumerate all the vertices of a polytope \mathcal{B}

- 1: **for** $i = 1, 2, \dots, S$ **do**
 - 2: Obtain vertex set \mathcal{V}_s by applying Algorithm 2 to \mathcal{B}_s
 - 3: **end for**
 - 4: Generate vertices \mathbf{b}^v for \mathcal{B} by concatenating all the individual vertices \mathbf{b}_s as $\mathbf{b}^v = [(\mathbf{b}'_1)^v, \dots, (\mathbf{b}'_S)^v]'$, $\mathbf{b}_s \in \mathcal{V}_s$
-

all the RES facilities. Then, concatenate the obtained vertices to get the ones for each RES facility by Step 4 in Algorithm 3. Finally, run this step again to form the vertices of (4) by concatenating the vertices of each \mathcal{W}_i .

- ii) For uncertainty sets (6), use Algorithm 2 to obtain the vertices for each sub-horizon \mathcal{T}_s . Note that concatenating step in Algorithm 3 is not needed in this case because problem (25) is decomposable across sub-horizons \mathcal{T}_s , $s = 1, \dots, S$, and can be independently solved accordingly.

After the detailed description of vertex enumerating procedures for RES uncertainty sets, a discussion on the complexity of solving (25) follows.

Remark 2. (*Complexity of solving (25)*). Vertex enumeration incurs exponential complexity because the number of vertices can increase exponentially with the number of variables and constraints [28, Ch. 2]. However, if the cardinality of each sub-horizon \mathcal{T}_s is not very large (e.g., when 24 hours are partitioned into 4 sub-horizons each comprising 6 time slots), then the complexity is affordable. Most importantly, the vertices of \mathcal{W} need only be listed once, before optimization.

IV. NUMERICAL TESTS

In this section, numerical results are presented to verify the performance of the robust and distributed energy scheduler. The considered microgrid consists of $M = 3$ conventional generators, $N = 6$ class \mathcal{K}_1 dispatchable loads, $Q = 6$ class \mathcal{K}_2 dispatchable loads, $J = 3$ storage devices, and $I = 2$ renewable energy facilities (wind farms). The time horizon spans $T = 8$ hours, corresponding to the interval 4pm-12am. The generation costs $C_m(P_{G_m}) = a_m P_{G_m}^2 + b_m P_{G_m}$ and the utilities of class \mathcal{K}_1 elastic loads $U_n(P_{D_n}) = c_n P_{D_n}^2 + d_n P_{D_n}$ are set to be quadratic and time-invariant. Generator parameters are given in Table I and $\text{SR}^t = 10\text{kWh}$. The relevant parameters of two classes of dispatchable loads are depicted in Tables II and III (see also [3], [4], and [26]). The utility of class \mathcal{K}_2 loads is $U_{E_q}^t(P_{E_q}^t) := \pi_q^t P_{E_q}^t$ with weights $\pi_q^t = 4, 3.5, \dots, 1, 0.5$ for $t = 4\text{pm}, \dots, 11\text{am}$ and $q \in \mathcal{Q}$.

Three batteries have capacity $B_j^{\max} = 30\text{kWh}$ (similar to [9]). The remaining parameters are $P_{B_j}^{\min} = -10\text{kWh}$, $P_{B_j}^{\max} = 10\text{kWh}$, $B_j^{\min} = 5\text{kWh}$, and $\eta_j^{\text{dis}} = \eta_j^{\text{ch}} = 0.9$, for all $j \in \mathcal{J}$. The penalty weights for $t = 4\text{pm}, \dots, 11\text{am}$ are set as $\varpi_1^t = 0.05, 0.1, \dots, 0.35, 0.4$ and $\varpi_j^t = 0.1$, $j = 2, 3$, $t \in \mathcal{T}$. The joint uncertainty model with $S = 1$ is considered for \mathcal{W} [cf. (6)], where $W_1^{\min} = 40\text{kWh}$, and $W_1^{\max} = 360\text{kWh}$. In order to obtain \underline{W}_i^t and \bar{W}_i^t listed in Table IV, MISO day ahead wind forecast data [29] are rescaled to the order of 1 kWh to 40 kWh, which is a typical wind power generation for a microgrid [16].

TABLE I

GENERATING CAPACITIES, RAMPING POWER, AND COST COEFFICIENTS. THE UNITS OF a_m AND b_m ARE $\$/(\text{kWh})^2$ AND $\$/\text{kWh}$, RESPECTIVELY.

Unit	$P_{G_m}^{\min}$	$P_{G_m}^{\max}$	$R_{m,\text{up(down)}}$	a_m	b_m
1	10	50	40	0.006	0.5
2	8	45	40	0.003	0.25
3	15	70	40	0.004	0.3

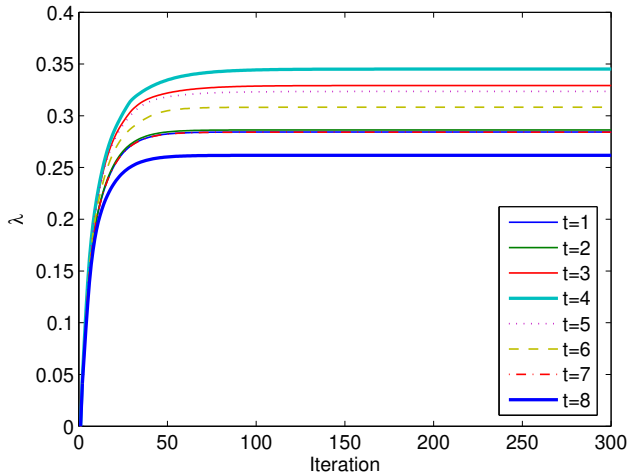
TABLE II

CLASS \mathcal{K}_1 DISPATCHABLE LOADS PARAMETERS. THE UNITS OF c_n AND d_n ARE $\$/(\text{kWh})^2$ AND $\$/\text{kWh}$, RESPECTIVELY.

\mathcal{K}_1	Load 1	Load 2	Load 3	Load 4	Load 5	Load 6
$P_{D_n}^{\min}$	0.5	4	2	5.5	1	7
$P_{D_n}^{\max}$	10	16	15	20	27	32
c_n	0.002	0.0011	0.003	0.0024	0.0015	0.0037
d_n	0.2	0.11	0.3	0.24	0.15	0.37

Similarly, the fixed load L^t in Table V is a rescaled version of the cleared load provided by MISO's daily report [30]. For the transaction prices, two different cases are studied as given in Table V, where $\{\alpha^t\}$ in Case A are real-time prices of the Minnesota hub in MISO's daily report. To evaluate the effect of high transaction prices, $\{\alpha^t\}$ in Case B is set as 20 times of that in Case A. For both cases, $\beta^t = 0.9\alpha^t$, which satisfies the convexity condition for (P1) given in Proposition 1.

First, convergence of the Lagrange multiplier $\{\lambda^t\}$ corresponding to the balance equation (8o) is confirmed for Case A by Fig. 3. It can be seen that λ^t converges for all $t \in \mathcal{T}$ within a couple of hundred iterations, which verifies the validity of the dual decomposition approach using the subgradient projection method. With the running averages, convergence of the other dual and primal variables was also verified (for Case B too), but is omitted for brevity.

Fig. 3. Convergence of $\{\lambda^t\}$.

The optimal microgrid power schedules of two cases are shown in Figs. 4 and 5. The staircase curves include $P_G^t := \sum_m P_{G_m}^t$, $P_D^t = \sum_n P_{D_n}^t$, and $P_E^t = \sum_q P_{E_q}^t$ denoting the total conventional power generation, and total elastic demand for classes \mathcal{K}_1 and \mathcal{K}_2 , respectively, which are the optimal solutions of (P2). Quantity W_{worst}^t denotes the total worst-case

TABLE III

CLASS \mathcal{K}_2 DISPATCHABLE LOADS PARAMETERS

\mathcal{K}_2	Load 1	Load 2	Load 3	Load 4
$P_{E_q}^{\min}$	0	0	0	0
$P_{E_q}^{\max}$	1.2	1.55	1.3	1.7
E_q^{\max}	5	5.5	4	8
S_q	6pm	7pm	6pm	6pm
T_q	12am	11am	12am	12am

TABLE IV

LIMITS OF FORECASTED WIND POWER

Slot	1	2	3	4	5	6	7	8
W_1^t	2.47	2.27	2.18	1.97	2.28	2.66	3.1	3.38
\bar{W}_1^t	24.7	22.7	21.8	19.7	22.8	26.6	31	33.8
W_2^t	2.57	1.88	2.16	1.56	1.95	3.07	3.44	3.11
\bar{W}_2^t	25.7	18.8	21.6	15.6	19.5	30.7	34.4	31.1

wind energy at slot t , which is the optimal solution of (25) with optimal \tilde{P}_R^t .

A common observation from Figs. 4 and 5 is that the total conventional power generation P_G^t varies with the same trend across t as the fixed load demand L^t , while the \mathcal{K}_1 elastic load exhibits the opposite trend. Because the conventional generation and the power drawn from the main grid are limited, the optimal scheduling by solving (P2) dispatches less power for P_D^t when L^t is large (from 6PM to 9PM), and vice versa. This behavior indeed reflects the load shifting ability of the proposed design for the microgrid energy management. Due to the starting time S_q (cf. Table III), another fact for both cases is the zero power scheduling of P_E^t for the time period of 4PM to 6PM, and the decreasing trend of P_E^t after 6PM. Further elaboration on the behavior of each $P_{E_q}^t$ is provided later.

Furthermore, by comparing two cases in Figs. 4 and 5, it is interesting to illustrate the effect of the transaction prices. Remember that the difference between \tilde{P}_R^t and W_{worst}^t is the shortage power needed to purchase (if positive) or the surplus power to be sold (if negative), Figs. 4 shows that the microgrid always purchases energy from the main grid because \tilde{P}_R^t is more than W_{worst}^t . This is because for Case A, the purchase price α^t is much lower than the marginal cost of the conventional generation (cf. Tables I and V). The economic scheduling decision is thus to reduce conventional generation while purchasing more power to keep the supply-demand balance. For Case B, since α^t is much higher than that in Case A, less power should be purchased which is reflected in the relatively small gap between \tilde{P}_R^t and W_{worst}^t across time slots. It can also be seen that \tilde{P}_R^t is smaller than W_{worst}^t from 7PM to 8PM, meaning that selling activity happens and is encouraged by the highest selling price β^t in this slot across the entire time horizon. Moreover, selling activity results in the peak conventional generation from 7PM to 8PM. Fig. 6 compares the optimal costs for the two cases. It can be seen that the optimal costs of conventional generation and worst-case transaction of Case B are higher than those of Case A, which can be explained by the higher transaction prices and the resultant larger DG output for Case B.

TABLE V
FIXED LOADS DEMAND AND TRANSACTION PRICES. THE UNITS OF α^t
AND β^t ARE ¢/kWh .

Slot	1	2	3	4	5	6	7	8
L^t	57.8	58.4	64	65.1	61.5	58.8	55.5	51
(Case A)								
α^t	2.01	2.2	3.62	6.6	5.83	3.99	2.53	2.34
β^t	1.81	1.98	3.26	5.94	5.25	3.59	2.28	2.11
(Case B)								
α^t	40.2	44	72.4	132	116.6	79.8	50.6	46.8
β^t	36.18	39.6	65.16	118.8	104.94	71.82	45.54	42.12

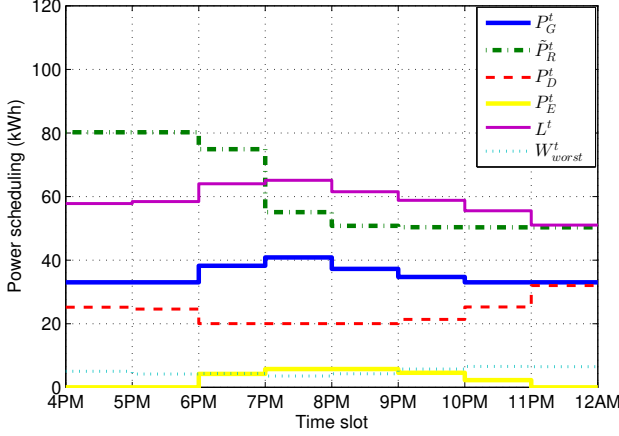


Fig. 4. Optimal power schedules: Case A.

The optimal power scheduling of class \mathcal{K}_2 elastic load is depicted in Fig. 7 for Case A. The decreasing trend for all the \mathcal{K}_2 loads is due to the decreasing weights $\{\pi_q^t\}$ from S_q to T_q , which is established from the fast charging motivation for the PHEVs, for example.

Fig. 8 depicts the optimal SoC of the battery storage devices for Case A. The coincidence of SoC and the battery capacity for the several last slots is the result of the postulated battery cost penalizing the deviation from capacity. The increasing SoC behavior can be explained by the increasing weights $\{\varpi_j^t\}$.

Fig. 9 shows the effect of different selling prices $\{\beta^t\}$ on the optimal energy costs, where Case B is studied with fixed purchase prices $\{\alpha^t\}$. It can be clearly seen that the net cost decreases with the increase of the selling-to-purchase-price ratio β^t/α^t . When this ratio increases, the microgrid has a higher margin for revenue from the transaction mechanism, which yields the reduced worst-case transaction cost. Finally, it is worth mentioning that if a similar numerical test was implemented for Case A, but no significant change emerged in either type of cost. The reason is that the low real-time prices $\{\alpha^t\}$ and $\{\beta^t\}$ in Case A do not considerably affect the transaction amount for different selling prices.

V. CONCLUSIONS AND FUTURE WORK

A distributed energy management approach was developed tailored for microgrids with high penetration of renewable energy sources. By introducing the notion of committed renewable energy, a novel model was introduced to deal

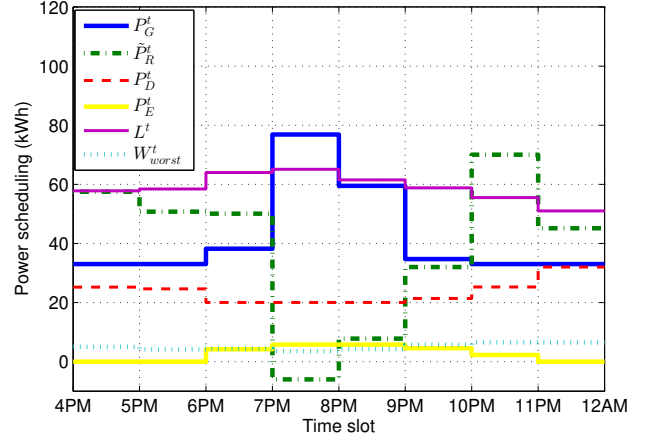


Fig. 5. Optimal power schedules: Case B.

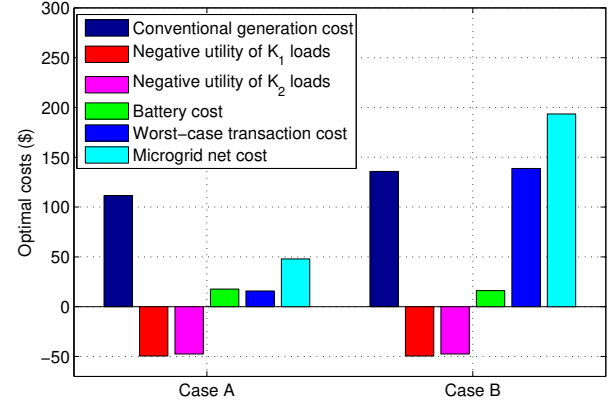


Fig. 6. Optimal costs: Case A and B.

with the challenging constraint of the supply-demand balance raised by the intermittent nature of renewable energy sources. Not only the conventional generation costs, utilities of the adjustable loads, and distributed storage costs were accounted for, but also the worst-case transaction cost was included in the objective. To schedule power in a distributed fashion, the dual decomposition method was utilized to decompose the original problem into smaller subproblems solved by the LCs of conventional generators, dispatchable loads, DS devices and the RES. The numerical tests demonstrated the optimal power generated, consumed by and delivered to the DERs, and the controllable loads across the entire time horizon.

A number of interesting research directions open up towards extending the model and approach proposed in this paper. Some classical but fundamental problems, such as the optimal power flow (OPF) and the unit commitment (UC) problems are worth re-investigating with the envisaged growth of RES usage in microgrids.

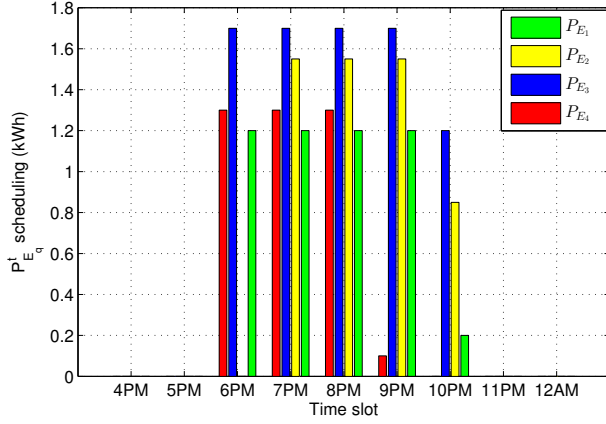


Fig. 7. Optimal power schedule for $P_{E_q}^t$: Case A.

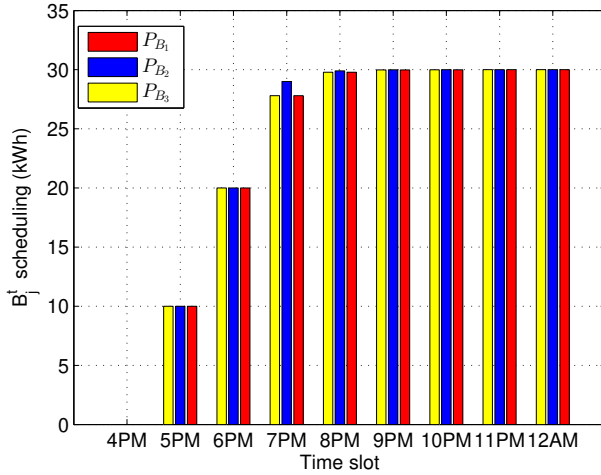


Fig. 8. Optimal power schedule for B_j^t : Case A.

APPENDIX I ENHANCING THE BUNDLE METHOD

Using an auxiliary variable r , (26) can be re-written as

$$\min_{\mathbf{p}, r} \quad r + \frac{\rho\ell}{2} \|\mathbf{p} - \mathbf{y}_\ell\|^2 \quad (28a)$$

$$\text{s.t.} \quad \tilde{G}(\mathbf{p}_i) + \mathbf{g}'_i(\mathbf{p} - \mathbf{p}_i) \leq r, \quad i = 0, 1, \dots, \ell. \quad (28b)$$

Introducing multipliers $\boldsymbol{\xi} \in \mathbb{R}_+^{\ell+1}$, the Lagrangian is given as

$$\begin{aligned} \mathcal{L}(r, \mathbf{p}, \boldsymbol{\xi}) = & \left(1 - \sum_{i=0}^{\ell+1} \xi_i\right) r + \frac{\rho\ell}{2} \|\mathbf{p} - \mathbf{y}_\ell\|^2 \\ & + \sum_{i=0}^{\ell+1} \xi_i (\tilde{G}(\mathbf{p}_i) + \mathbf{g}'_i(\mathbf{p} - \mathbf{p}_i)). \end{aligned} \quad (29)$$

Optimality condition on \mathbf{p} , i.e., $\nabla_{\mathbf{p}} \mathcal{L}(r, \mathbf{p}, \boldsymbol{\xi}) = \mathbf{0}$, yields

$$\mathbf{p}^* = \mathbf{y}_\ell - \frac{1}{\rho\ell} \sum_{i=0}^{\ell+1} \xi_i \mathbf{g}_i. \quad (30)$$

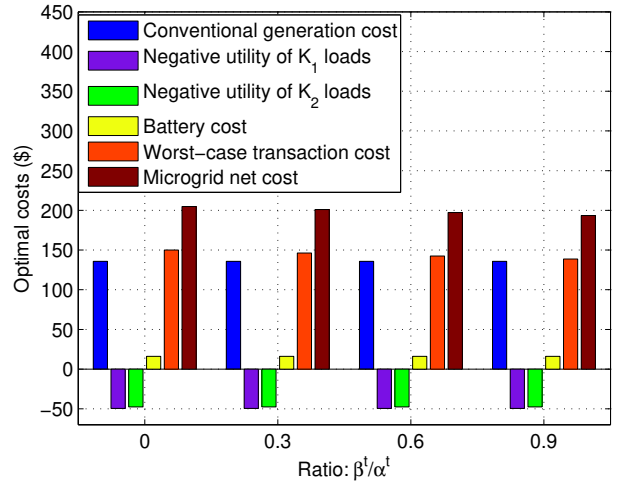


Fig. 9. Optimal costs: Case B.

Substituting (30) into (29), the dual of (28) is

$$\max_{\boldsymbol{\xi}} \quad -\frac{1}{2\rho\ell} \left\| \sum_{i=0}^{\ell+1} \xi_i \mathbf{g}_i \right\|^2 + \sum_{i=0}^{\ell+1} \xi_i (\tilde{G}(\mathbf{p}_i) + \mathbf{g}'_i(\mathbf{y}_\ell - \mathbf{p}_i)) \quad (31a)$$

$$\text{s.t.} \quad \boldsymbol{\xi} \succeq \mathbf{0}, \quad \mathbf{1}'\boldsymbol{\xi} = 1 \quad (31b)$$

where $\mathbf{1}$ is the all-ones vector.

Note that (31) is essentially a QP over the simplex in $\mathbb{R}^{\ell+1}$, which can be solved very efficiently.

APPENDIX II PROOFS OF PROPOSITIONS

To prove Propositions 3 and 4, the following lemma is needed, which shows sufficient and necessary conditions for a point to be a vertex of a polytope represented as a linear system [31, Sec. 3.5].

Lemma 1. *For a polytope $\mathcal{P} := \{\mathbf{x} \in \mathbb{R}^n | \mathbf{A}\mathbf{x} \preceq \mathbf{c}\}$, a point $\mathbf{v} \in \mathcal{P}$ is a vertex if and only if there exists a subsystem $\tilde{\mathbf{A}}\mathbf{x} \preceq \tilde{\mathbf{c}}$ of $\mathbf{A}\mathbf{x} \preceq \mathbf{c}$ so that $\text{rank}(\tilde{\mathbf{A}}) = n$ and \mathbf{v} is the unique (feasible) solution of $\tilde{\mathbf{A}}\mathbf{v} = \tilde{\mathbf{c}}$.*

A. Proof of Proposition 3

The polytope $\mathcal{A} := \{\mathbf{a} \in \mathbb{R}^n | \underline{\mathbf{a}} \preceq \mathbf{a} \preceq \bar{\mathbf{a}}, a^{\min} \leq \mathbf{1}'\mathbf{a} \leq a^{\max}\}$ can be re-written as $\mathcal{A} := \{\mathbf{a} \in \mathbb{R}^n | \mathbf{A}\mathbf{a} \preceq \mathbf{c}\}$, where $\mathbf{A} := [\mathbf{I}_{n \times n}, -\mathbf{I}_{n \times n}, \mathbf{1}, -\mathbf{1}]'$ and $\mathbf{c} := [\bar{\mathbf{a}}', -\underline{\mathbf{a}}', a^{\max}, -a^{\min}]'$. By Lemma 1, enumerating vertices of \mathcal{A} is equivalent to finding all feasible solutions of the linear subsystems $\tilde{\mathbf{A}}\mathbf{a} = \tilde{\mathbf{c}}$, such that rank- n matrix $\tilde{\mathbf{A}}$ is constructed by extracting rows of \mathbf{A} . It can be seen that such full column-rank matrix $\tilde{\mathbf{A}}$ can only have two forms (with row permutation if necessary): i) $\tilde{\mathbf{A}}_1 = \text{diag}(\mathbf{d})$ with $d_i \in \{-1, 1\}$, $i = 1, \dots, n$; ii) $\tilde{\mathbf{A}}_2(i, :) = \pm \mathbf{1}'$, $i = 1, \dots, n$, and $\tilde{\mathbf{A}}_2(j, :) = \tilde{\mathbf{A}}_1(j, :)$, $\forall j \neq i$. Basically, $\tilde{\mathbf{A}}_1$ is constructed by choosing n vectors as a basis of \mathbb{R}^n from the first $2n$ rows of \mathbf{A} . Substituting any row of $\tilde{\mathbf{A}}_1$ with $\pm \mathbf{1}'$, forms $\tilde{\mathbf{A}}_2$. Finally, by solving all the linear subsystems of the form $\tilde{\mathbf{A}}_k \mathbf{a} = \tilde{\mathbf{c}}_k$, for $k = 1, 2$, Proposition 3 follows readily.

B. Proof of Proposition 4

The polytope $\mathcal{B} := \{\mathbf{b} \in \mathbb{R}^n \mid \underline{\mathbf{b}} \preceq \mathbf{b} \preceq \bar{\mathbf{b}}, b_s^{\min} \leq \mathbf{1}'_{n_s} \mathbf{b}_s \leq b_s^{\max}, s = 1, \dots, S\}$ can be re-written as $\mathcal{B} := \{\mathbf{b} \in \mathbb{R}^n \mid \mathbf{B}\mathbf{b} \preceq \mathbf{c}\}$, where $\mathbf{B} := \text{diag}(\mathbf{B}_1, \dots, \mathbf{B}_S)$, $\mathbf{c} := [\mathbf{c}'_1, \dots, \mathbf{c}'_S]'$, $\mathbf{B}_s := [\mathbf{I}_{n_s \times n_s}, -\mathbf{I}_{n_s \times n_s}, \mathbf{1}, -\mathbf{1}]'$, and $\mathbf{c}_s := [\bar{\mathbf{a}}'_s, -\underline{\mathbf{a}}'_s, b_s^{\max}, -b_s^{\min}]'$ for $s = 1, \dots, S$.

Similarly by Lemma 1, all the vertices of \mathcal{B} can be enumerated by solving $\tilde{\mathbf{B}}\mathbf{b} = \tilde{\mathbf{c}}$, where the rank- n matrix $\tilde{\mathbf{B}}$ is formed by extracting rows of \mathbf{B} . Due to the block diagonal structure of \mathbf{B} , it can be seen that the only way to find its n linear independent rows is to find n_s linear independent vectors from the rows corresponding to \mathbf{B}_s for $s = 1, \dots, S$. In other words, the vertices \mathbf{b}^v can be obtained by concatenating all the individual vertices \mathbf{b}_s as stated in Proposition 4.

REFERENCES

- [1] N. Hatziargyriou, H. Asano, R. Iravani, and C. Marnay, "Microgrids: An overview of ongoing research, development, and demonstration projects," *IEEE Power & Energy Mag.*, vol. 5, no. 4, pp. 78–94, July–Aug. 2007.
- [2] P. Stluka, D. Godbole, and T. Samad, "Energy management for buildings and microgrids," in *Proc. of the 50th IEEE Conf. on Decision and Control and European Control Conf.*, Orlando, FL, Dec. 12–15, 2011.
- [3] S. Choi, S. Park, D.-J. Kang, S.-J. Han, and H.-M. Kim, "A microgrid energy management system for inducing optimal demand response," in *Proc. of the 2nd Intl. Conf. Smart Grid Communications*, Brussels, Belgium, Oct. 17–20, 2011.
- [4] A. Parisio and L. Glielmo, "A mixed integer linear formulation for microgrid economic scheduling," in *Proc. of the 2nd Intl. Conf. Smart Grid Communications*, Brussels, Belgium, Oct. 17–20, 2011.
- [5] R. Palma-Behnke, C. Benavides, E. Aranda, J. Llanos, and D. Sáez, "Energy management system for a renewable based microgrid with a demand side management mechanism," in *Proc. of IEEE Symp. on Comput. Intell. Apps. in Smart Grid*, Paris, France, Apr. 11–15, 2011.
- [6] J. Hetzer, C. Yu, and K. Bhattacharai, "An economic dispatch model incorporating wind power," *IEEE Trans. on Energy Convers.*, vol. 23, no. 2, pp. 603–611, June 2008.
- [7] M. J. Neely, A. S. Tehrani, and A. G. Dimakis, "Efficient algorithms for renewable energy allocation to delay tolerant consumers," in *Proc. of the 1st Intl. Conf. Smart Grid Communications*, Gaithersburg, MD, Oct. 4–6, 2010.
- [8] X. Liu and W. Xu, "Economic load dispatch constrained by wind power availability: A here-and-now approach," *IEEE Trans. on Sustainable Energy*, vol. 1, no. 1, pp. 2–9, Apr. 2010.
- [9] X. Guan, Z. Xu, and Q.-S. Jia, "Energy-efficient buildings facilitated by microgrid," *IEEE Trans. on Smart Grid*, vol. 1, no. 3, pp. 243–252, Dec. 2010.
- [10] D. Bertsimas, E. Litvinov, X. Sun, J. Zhao, and T. Zheng, "Adaptive robust optimization for the security constrained unit commitment problem," Mar. 2011, [Online]. Available: http://web.mit.edu/sunx/www/Adaptive_Robust_UC_Revision.pdf.
- [11] L. Jiang and S. H. Low, "Real-time demand response with uncertain renewable energy in smart grid," in *Proc. of the 49th Allerton Conf. on Comm., Control, and Computing*, Monticello, IL, Sept. 2011, pp. 1334–1341.
- [12] L. Zhao and B. Zeng, "Robust unit commitment problem with demand response and wind energy," Univ. of S. Florida, Tech. Rep., Oct. 2010, [Online]. Available: http://www.optimization-online.org/DB_FILE/2010/11/2784.pdf.
- [13] C. Jin and P. K. Ghosh, "Coordinated usage of distributed sources for energy cost saving in micro-grid," in *Proc. of the 43rd North American Power Symposium (NAPS)*, Boston, MA, Aug. 4–6, 2011.
- [14] K. M. Chandy, S. H. Low, U. Topcu, and H. Xu, "A simple optimal power flow model with energy storage," in *Proc. of the 49th IEEE Conf. on Decision and Control*, Atlanta, GA, Dec. 15–17, 2010.
- [15] W. Saad, Z. Han, H. V. Poor, and T. Başar, "Game theoretic methods for the smart grid," Feb. 2012, [Online]. Available: <http://arxiv.org/abs/1202.0452>.
- [16] C. Wu, H. Mohsenian-Rad, J. Huang, and Y. Wang, "Demand side management for wind power integration in microgrid using dynamic potential game theory," in *Proc. of 2011 IEEE GLOBECOM Workshops*, Houston, TX, Dec. 5–9, 2011.
- [17] A. D. Domínguez-García and C. N. Hadjicostis, "Distributed algorithms for control of demand response and distributed energy resources," in *Proc. of the 50th IEEE Control and Decision Conf.*, Orlando, FL, Dec. 2011.
- [18] P. Pinson and G. Kariniotakis, "Conditional prediction intervals of wind power generation," *IEEE Trans. on Power Systems*, vol. 25, no. 4, pp. 1845–1856, Nov. 2010.
- [19] J. A. Carta, P. Ramírez, and S. Velázquez, "A review of wind speed probability distributions used in wind energy analysis: Case studies in the canary islands," *Renewable and Sustainable Energy Reviews*, vol. 13, pp. 933–955, 2009.
- [20] S. Boyd and L. Vandenberghe, *Convex Optimization*. Cambridge University Press, 2004.
- [21] D. P. Bertsekas, *Nonlinear Programming*, 2nd ed. Belmont, MA: Athena Scientific, 1999.
- [22] A. J. Conejo, E. Castillo, R. Mínguez, and R. García-Bertrand, *Decomposition Techniques in Mathematical Programming: Engineering and Science Applications*. Springer, 2006.
- [23] D. Palomar and M. Chiang, "A tutorial on decomposition methods for network utility maximization," *IEEE J. Sel. Areas Commun.*, vol. 46, no. 8, pp. 1439–1451, Aug. 2006.
- [24] D. P. Bertsekas, *Convex Optimization Theory*. Belmont, MA: Athena Scientific, 2009.
- [25] A. Nedić and A. Ozdaglar, "Approximate primal solutions and rate analysis for dual subgradient methods," *SIAM J. Optim.*, vol. 19, no. 4, pp. 1757–1780, 2009.
- [26] N. Gatsis and G. B. Giannakis, "Residential load control: Distributed scheduling and convergence with lost AMI messages," *IEEE Trans. on Smart Grid*, vol. 3, no. 2, pp. 770–786, June 2012.
- [27] S. Feltenmark and K. C. Kiwiel, "Dual application of proximal bundle methods, including Lagrange relaxation of nonconvex problems," *SIAM J. Optim.*, vol. 10, no. 3, pp. 697–721, Feb./Mar. 2000.
- [28] D. Bertsimas and J. N. Tsitsiklis, *Introduction to Linear Optimization*. Belmont, MA: Athena Scientific, 1997.
- [29] MISO Market Data, [Online]. Available: <https://www.midwestiso.org/MarketsOperations/RealTimeMarketData/Pages/DayAhead>
- [30] Federal Energy Regulatory Commission, "MISO daily report," Feb. 29, 2012, [Online]. Available: <http://www.ferc.gov/market-oversight/mkt-electric/midwest/miso-rto-dly-rpt.pdf>.
- [31] U. Faigle, W. Kern, and G. Still, *Algorithmic Principles of Mathematical Programming*. Norwell, MA: Kluwer Academic Publishers, 2002.